JOURNAL OF GEOPHYSICAL RESEARCH, VOL. 103, NO. A8, PAGES 17,691–17,700, AUGUST 1, 1998

Magnetopause location under extreme solar wind conditions

J.-H. Shue,[1] P. Song,[2] C. T. Russell,[3] J. T. Steinberg,[4] J. K. Chao,[5] G. Zastenker,[6] O. L. Vaisberg,[6] S. Kokubun,[1] H. J. Singer,[7] T. R. Detman,[7] and H. Kawano[1,8]

Abstract. During the solar wind dynamic pressure enhancement, around 0200 UT on January 11, 1997, at the end of the January 6-11 magnetic cloud event, the magnetopause was pushed inside geosynchronous orbit. The LANL 1994-084 and GMS 4 geosynchronous satellites crossed the magnetopause and moved into the magnetosheath. Also, the Geotail satellite was in the magnetosheath while the Interball 1 satellite observed magnetopause crossings. This event provides an excellent opportunity to test and validate the prediction capabilities and accuracy of existing models of the magnetopause location for producing space weather forecasts. In this paper, we compare predictions of two models: the *Petrinec and Russell* [1996] model and the *Shue et al.* [1997] model. These two models correctly predict the magnetopause crossings on the dayside; however, there are some differences in the predictions along the flank. The *Shue et al.* [1997] model correctly predicts the Geotail magnetopause crossings and partially predicts the Interball 1 crossings. The *Petrinec and Russell* [1996] model correctly predicts the Interball 1 crossings and is partially consistent with the Geotail observations. We further found that some of the inaccuracy in Shue et al.'s predictions is due to the inappropriate linear extrapolation from the parameter range for average solar wind conditions to that for extreme conditions. To improve predictions under extreme solar wind conditions, we introduce a nonlinear dependence of the parameters on the solar wind conditions to represent the saturation effects of the solar wind dynamic pressure on the flaring of the magnetopause and saturation effects of the interplanetary magnetic field B_z on the subsolar standoff distance. These changes lead to a better agreement with the Interball 1 observations for this event.

1. Introduction

The location of the magnetopause is one of the most important parameters in space physics because it is the boundary that separates the magnetospheric plasma from the solar wind and determines the size of the magnetosphere. *Chapman and Ferraro* [1931] first introduced the concept of the magnetopause location which depends on the solar wind dynamic pressure (D_p). *Ferraro* [1952] first calculated the size of the magnetosphere and the shape of the magnetopause. Over the past few decades, space physicists have exerted much effort to model the location of the magnetopause under various solar wind conditions. In most of the early work, the location of the magnetopause depends solely on the solar wind dynamic pressure. Subsequently, *Fairfield* [1971] recognized that the interplanetary magnetic field (IMF) orientation can also affect the magnetopause location.

Later, more empirical models of the magnetopause location were developed using large in situ data sets of magnetopause crossings [*Howe and Binsack*, 1972; *Formisano et al.*, 1979; *Sibeck et al.*, 1991; *Petrinec et al.*, 1991; *Petrinec and Russell*, 1993, 1996; *Roelof and Sibeck*, 1993; *Shue et al.*, 1997]. Some of models [*Fairfield*, 1971; *Howe and Binsack*, 1972; *Formisano et al.*, 1979; *Petrinec et al.*, 1991; *Sibeck et al.*, 1991] define the magnetopause size and shape for each parameter range but are not valid for the broad, and especially extreme, ranges of solar wind conditions. The most recent empirical models [*Roelof and Sibeck*, 1993; *Petrinec and*

[1]Solar-Terrestrial Environment Laboratory, Nagoya University, Toyokawa, Japan.
[2]Space Physics Research Laboratory, University of Michigan, Ann Arbor.
[3]Institute of Geophysics and Planetary Physics, University of California, Los Angeles.
[4]Center for Space Research, Massachusetts Institute of Technology, Cambridge.
[5]Institute of Space Science, National Central University, Chungli, Taiwan.
[6]Space Research Institute, Russian Academy of Sciences, Moscow.
[7]National Oceanic and Atmospheric Administration, Space Environment Center, Boulder, Colorado.
[8]Now at Department of Earth and Planetary Sciences, Kyushu University, Hakozaki, Fukuoka, Japan.

Copyright 1998 by the American Geophysical Union.

Paper number 98JA01103.
0148-0227/98/98JA-01103$09.00

Russell 1996; *Shue et al.*, 1997] provide mathematical expressions for the size and shape of the magnetopause as functions of the north-south component of the IMF and the solar wind dynamic pressure. An important consequence emerging from these new models is that the magnetopause becomes predictable for any given upstream conditions. In this study, we compare predictions from the *Petrinec and Russell* [1996] model and the *Shue et al.* [1997] model with in situ observations for a particular event. We are not comparing with the *Roelof and Sibeck* [1993] model because our test conditions are outside the stated range of validity of the model.

These two models assume cylindric symmetry around the aberrated Sun-Earth line and have been derived with data sets that are for normal, rather than extreme, solar wind conditions. Both *Shue et al.* [1997] and *Petrinec and Russell* [1996] claim their models are valid over a wide solar wind parameter range. The detailed information about the databases and methods used to derive the two models will be discussed in section 2.

A magnetic cloud arrived at Earth on January 10-11, 1997. During this event, at 1115 UT on January 11, there was a failure of a geosynchronous communication satellite (Telstar 401). Also, as shown in Figure 1, during this event, around 0200 UT on January 11, while the interplanetary magnetic field was extremely strong and northward (~18 nT), there was a sudden enhancement in the solar wind dynamic pressure up to 60 nPa (including the contribution from helium ions). The magnetopause was pushed inside geosynchronous orbit because of the strong compression during this pressure enhancement which was 30 times more than the average solar wind dynamic pressure. Many satellites (LANL 1994-084, GMS 4, Geotail, and Interball 1) observed magnetopause crossings during this interval. Thus this event provides an excellent opportunity to test and validate the prediction capabilities and accuracy of existing empirical models of the magnetopause location for both space weather purposes and improving our scientific understanding. As will be shown in section 3, the two models provide similar magnetopause locations on the dayside; however, the predictions on the nightside are different under extreme solar wind conditions.

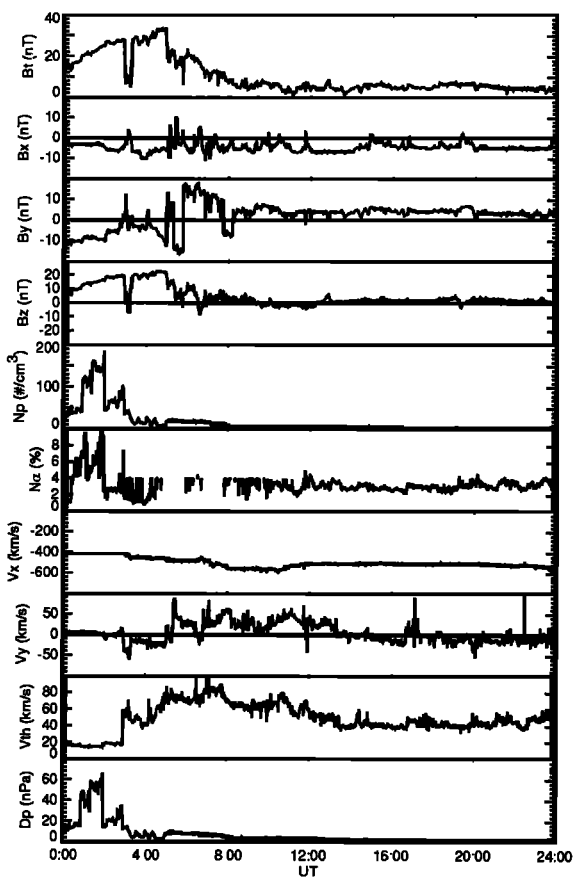

Figure 1. Magnetic field (**B**) and plasma data from the WIND satellite on January 11, 1997, in GSM coordinates. The solar wind dynamic pressure (D_p) includes the helium contribution by a factor ($1+0.04N_\alpha$), where N_α is the He^{++} concentration (an average value of 4% is used when N_α is missing). The V_{th} is the thermal speed of the solar wind.

2. Summary and Comparison of the Two Models

From a mathematical point of view, the models developed by *Shue et al.* [1997] and *Petrinec and Russell* [1996] were derived from best fits to observed magnetopause locations. The major differences are the databases, the functional form of the magnetopause, and the specific dependence of the magnetopause on the upstream solar wind.

2.1. Shue et al. [1997] Model

On the basis of a database of crossings from ISEE 1 and 2, AMPTE/IRM, and IMP 8 satellites, the locations of the magnetopause were fit to the functional form

$$r = r_0\left(\frac{2}{1+\cos\theta}\right)^{\alpha}, \tag{1}$$

where r is the radial distance and θ is the solar zenith angle. The positions X_s and R_s (subscript s denotes the *Shue et al.* [1997] model) are calculated by $X_s = r\cos\theta$ and $R_s = r\sin\theta$. This form has two parameters, r_0 and α, representing the standoff distance at the subsolar point and the level of tail flaring, respectively. A very important feature of this functional form is that the tail magnetopause can be either open (r goes to infinity when $\theta = \pi$) or closed (r approaches a finite value when $\theta = \pi$), depending on the value of α. Almost all other models used an elliptic equation as the basic functional form. Since an ellipse must close at some point on the nightside, it cannot represent the magnetopause for an open magnetosphere [*Fairfield*, 1995]. Both r_0 and α depend on the IMF B_z (in nanoteslas) and the solar wind dynamic pressure D_p (in nanopascals). Using a bivariant best fit, *Shue et al.* [1997] obtained

$$r_0 = \begin{cases} (11.4 + 0.013B_z)(D_p)^{-\frac{1}{6.6}}, & \text{for } B_z \geq 0 \\ (11.4 + 0.14B_z)(D_p)^{-\frac{1}{6.6}}, & \text{for } B_z < 0 \end{cases} \tag{2}$$

$$\alpha = (0.58 - 0.010B_z)(1 + 0.010D_p). \quad (3)$$

From these relations, the dependence of r_0 on the IMF B_z changes at $B_z = 0$ nT. A greater slope for the southward IMF reflects the erosion of the magnetopause associated with dayside reconnection. More magnetic flux is removed from the dayside and added to the nightside when the IMF is southward, and α increases. For northward IMF, high-latitude reconnection may add magnetic flux back to the dayside magnetosphere [*Gosling et al.*, 1991; *Song and Russell*, 1992] and slightly increase the standoff distance. Variations in dynamic pressure also change r_0 and α. The parameters r_0 and D_p are related with a power law index -1/6.6, which is slightly different from the index -1/6 for a pure dipole geomagnetic field. The value of α is slightly larger for larger dynamic pressure. This model used 5-min average solar wind data of B_z and D_p for each individual crossing. The model is valid in the ranges -18 nT $< B_z <$ 15 nT and 0.5 nPa $< D_p <$ 8.5 nPa.

Using the above relationship, we can predict the magnetopause location for given B_z and D_p obtained by a solar wind monitor. The relationship is therefore useful for space weather forecasting. It can also be used for comparisons with numerical simulations or theoretical models of the magnetopause [*Sotirelis*, 1996; *Kartalev et al.*, 1996; *Elsen and Winglee*, 1997].

2.2. Petrinec and Russell [1996] Model

Petrinec et al. [1991] used magnetopause crossings from the ISEE missions [*Song et al.*, 1988] to determine the dayside magnetopause size and shape for northward and southward IMF. *Petrinec and Russell* [1993] inferred the position of the nightside magnetopause based on total pressure balance at the magnetopause. *Petrinec and Russell* [1996] combined their dayside magnetopause location model [*Petrinec et al.*, 1991] with their nightside model [*Petrinec and Russell*, 1993] with a smooth connection at the terminator. They also used 5-min average IMP 8 data to obtain corresponding solar wind conditions. The range of validity of their model is -10 nT $< B_z <$ 10 nT and 0.5 nPa $< D_p <$ 8 nPa. Their functional form on the dayside magnetopause was written as

$$r = \frac{14.63(\frac{D_p}{2.1})^{-\frac{1}{6}}}{[1 + (\frac{14.63}{10.3 + m_1 B_z} - 1)\cos\theta]}, \quad (4)$$

where $m_1 = 0$ for northward IMF and $m_1 = 0.16$ for southward IMF. The position X^d_{pr} and R^d_{pr} (subscript pr denotes the *Petrinec and Russell* [1996] model and superscript d denotes dayside) are calculated by $X^d_{pr} = r\cos\theta$ and $R^d_{pr} = r\sin\theta$.

The magnetopause location on the nightside was expressed in a different functional form. For a given nightside position X^n_{pr} (superscript n denotes nightside),

$$R^n_{pr} = \frac{-2}{0.085} \sqrt{\arcsin\sqrt{2.98(D_p)^{-0.524}\exp^{0.085X^n_{pr}}(0.152 - m_2B_z)} - \arcsin\sqrt{2.98(D_p)^{-0.524}(0.152 - m_2B_z)}} + 14.63(\frac{D_p}{2.1})^{-\frac{1}{6}}, \quad (5)$$

where $m_2 = 0.00137$ for northward IMF and $m_2 = 0.00644$ for southward IMF.

In their model, the dayside location does not depend on B_z for northward IMF. On the nightside, the magnetopause location depends weakly on positive B_z. For southward IMF, *Petrinec and Russell*'s [1996] flaring decreases rapidly as the dynamic pressure increases. This model applies best when $D_p > 1$ nPa.

2.3. Comparisons Between the Two Models

Figure 2 shows an example of the comparison between *Petrinec and Russell* [1996] and *Shue et al.* [1997]. These two models give similar magnetopause location near the subsolar region. They both predict a slightly smaller standoff distance for southward IMF than for northward IMF. The predictions become different on the nightside. For southward IMF, the *Petrinec and Russell* [1996] model has a less flared tail magnetopause

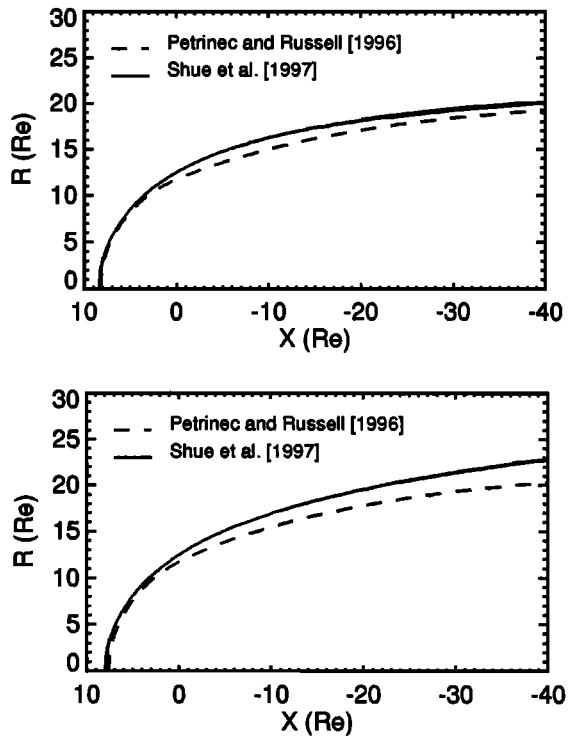

Figure 2. Comparison of *Petrinec and Russell* [1996] and *Shue et al.* [1997]. (top) Northward IMF (B_z = 5.0 nT and D_p = 8.0 nPa). (bottom) Southward IMF (B_z = -5.0 nT and D_p = 8.0 nPa). The vertical axis ($R = \sqrt{Y^2 + Z^2}$) is in aberrated GSM coordinates.

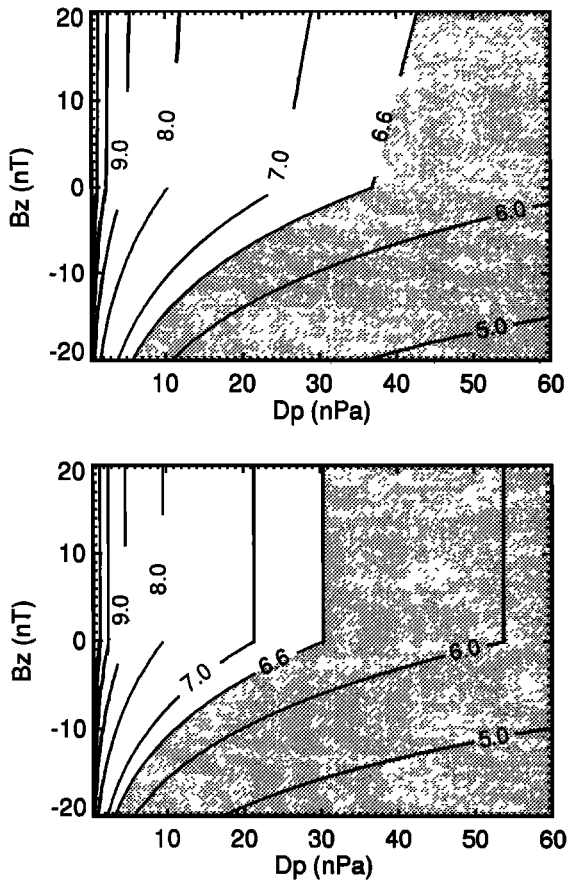

Figure 3. Comparison of the subsolar standoff distance r_0 between (top) *Shue et al.* [1997] and (bottom) *Petrinec and Russell* [1996]. The shaded (unshaded) region shows that r_0 is within (beyond) geosynchronous orbit.

than the *Shue et al.* [1997] model. The *Shue et al.* [1997] model predicts that the tail magnetopause is more flared for southward IMF than for northward IMF.

Figure 3 shows a general comparison of the subsolar standoff distance r_0 for these two models. The magnetopause location relative to geosynchronous orbit is of particular interest for space weather predictions because when the magnetopause moves within geosynchronous orbit, satellites at that location are exposed to magnetosheath particles and fields. The region within geosynchronous orbit is shaded in gray. Figure 3 (top) shows the subsolar standoff distance from *Shue et al.* [1997]; Figure 3 (bottom) is for *Petrinec and Russell* [1996]. We found that r_0 predicted by both models is within geosynchronous orbit (less than 6.6 R_E) for small D_p when the southward IMF is extremely strong. Note that Figure 3 shows the equilibrium r_0 for the corresponding values of B_z and D_p. The magnetopause may oscillate around the equilibrium value causing an uncertainty of about 0.5 R_E near the subsolar region [*Song et al.*, 1988].

3. Application to the January Event

Using values of B_z and D_p observed from the WIND satellite in Figure 1, we calculate the magnetopause location as a function of time. A time delay of 24 min has been taken into account for the arrival of the solar wind at the Earth. This time delay is calculated using the distance (~93 R_E) between the WIND satellite and Earth (early on January 11, 1997) divided by the solar wind speed (~410 km/s) under the assumption that the magnetopause is rigid and responds to solar wind conditions instantaneously. Figure 4 shows the locations of the magnetopause and various satellites at 0100 UT (B_z = 9.3 nT and D_p = 14.0 nPa). The solid and dashed curves represent the predictions by *Shue et al.* [1997] and *Petrinec and Russell* [1996], respectively. The difference between these two models is small on the dayside. Since in situ observations from Geotail indicate that it was in the magnetosheath during this time, both models succeed in the prediction.

We use these two models to calculate the distance between a satellite and a model magnetopause along the normal to the boundary as a function of time. Note that the solar wind aberration has been considered in these distance calculations. Figure 5 shows the calculated distances for the LANL 1994-084 satellite. A positive (negative) distance indicates that LANL 1994-084 was in the magnetosphere (magnetosheath). The predictions of these two models exhibit only small differences for this satellite. LANL 1994-084 data show that the satellite

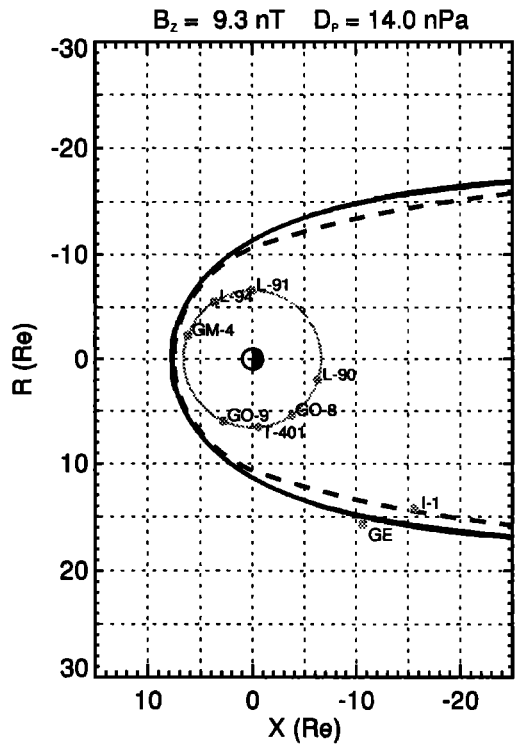

Figure 4. Locations of the magnetopause and satellites at 0100 UT on January 11, 1997. A solid curve is the prediction by *Shue et al.* [1997]; a dashed curve is predicted by *Petrinec and Russell* [1996]. Satellites are designated as follows: L-90, LANL 1990-095; L-91, LANL 1991-080; L-94, LANL 1994-084; GO-8, GOES 8; GO-9, GOES 9; GM-4, GMS 4; T-401, Telstar 401; GE, Geotail; I-1, Interball 1. The vertical axis ($R = \sqrt{Y^2 + Z^2}$) is in aberrated GSM coordinates.

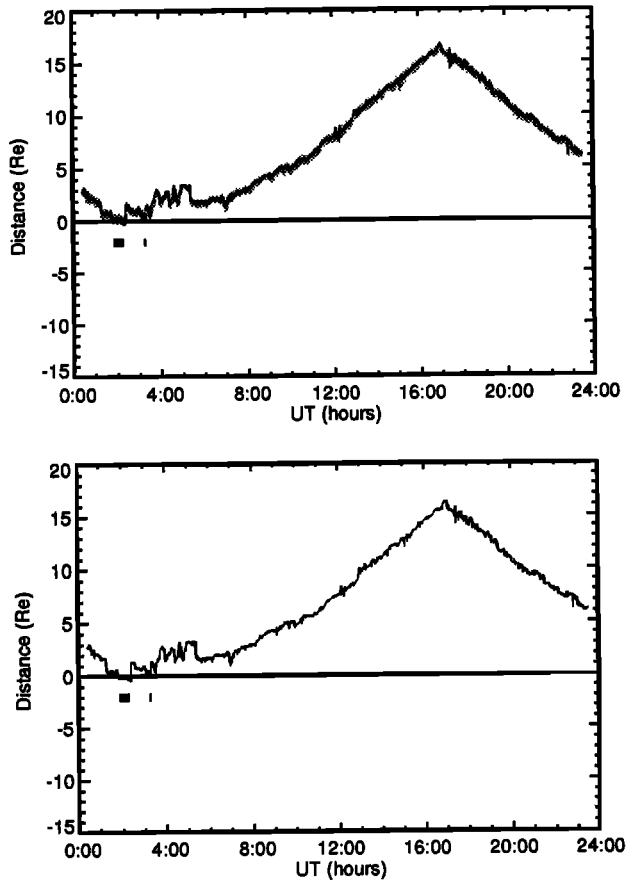

Figure 5. Distances between LANL 1994-084 and the magnetopause predicted by the two models as functions of time on January 11: (top) *Shue et al.* [1997] and (bottom) *Petrinec and Russell* [1996]. The distance is calculated as the smallest value from the satellite to the predicted magnetopause. A negative distance with a solid shading indicates that the satellite is in the magnetosheath. A positive distance shows that the satellite is in the magnetosphere. The uncertainty of the prediction estimated by *Shue et al.* [1997] is shaded in gray. Thick horizontal bars below the curves indicate periods when the satellite was in the magnetosheath according to the in situ measurements.

first crossed the magnetopause between 0152 and 0155 UT on January 11 and returned to the magnetosphere between 0217 and 0218 UT. There was a very brief period within the magnetosheath between 0313 and 0316 UT [*Thomsen et al.*, 1998]. Thick horizontal bars indicate the periods when the satellite was in the magnetosheath. These two models predict reasonably well the magnetopause location for this satellite, especially when the uncertainty of the distance calculation (gray region in Shue et al.) is taken into account. The uncertainty in the Shue et al. model is estimated by using coefficients with their standard deviations (by multiplying by a factor of $1/\sqrt{3}$) in Table 1 of *Shue et al.* [1997] to calculate half of the difference between the maximum and minimum magnetopause locations for each pair of B_z and D_p. The reason for multiplying by $1/\sqrt{3}$ is that *Shue et al.* [1997] randomly sampled one third of the total points (rather than the total number) to obtain the standard deviation. The uncertainty estimated when one randomly samples K points from a data set including N ($> K$) points is $\sqrt{N/K}$ times larger than the real uncertainty when one randomly samples N points. We note that the estimation error in the "corrected" quantity (by multiplying by $\sqrt{N/K}$) tends to increase with decreasing K. The uncertainty is calculated as functions of B_z, D_p, and solar zenith angle. To demonstrate the uncertainty, we choose $B_z = -4$ nT as an average value for southward IMF (dotted curve) and $B_z = 4$ nT as an average value for northward IMF (solid curve), as shown in Figure 6. For D_p, an average value of 2 nPa is used. It can be seen that the uncertainty increases rapidly with solar zenith angle, and the uncertainty for the southward IMF is larger than that for the northward IMF. This tendency is somewhat consistent with Figure 2 of *Song et al.* [1988], namely, the uncertainty could be mainly associated with the magnetopause oscillations.

The location of GMS 4 is more upstream than that of LANL 1994-084 during the large dynamic pressure enhancement. The GMS 4 measurements indicate that the satellite moved to the magnetosheath at 0115 UT (37 min earlier than LANL 1994-084 did) and moved back to the magnetosphere at 0218 UT (the same time as LANL 1994-084 did). Like LANL 1994-084, GMS 4 also had a short excursion to the magnetosheath at 0315 UT. Figure 7 shows the distance from GMS 4 to the predicted magnetopause. Thick horizontal bars in Figure 7 show the magnetosheath periods. The two models predict reasonably well for this satellite.

When Telstar 401 was lost at 1115 UT, the solar wind conditions had returned to near normal values. The magnetopause had moved outward to 8 R_E at the subsolar point, and Telstar 401 was far inside the magnetosphere when the malfunction occurred.

Figure 8 shows the distance to Geotail in the same format as Figure 5. Visual inspection of the particle distribution function data from the LEP instrument indicates that Geotail was located in the magnetosheath at the beginning of the day, made short excursions (last-

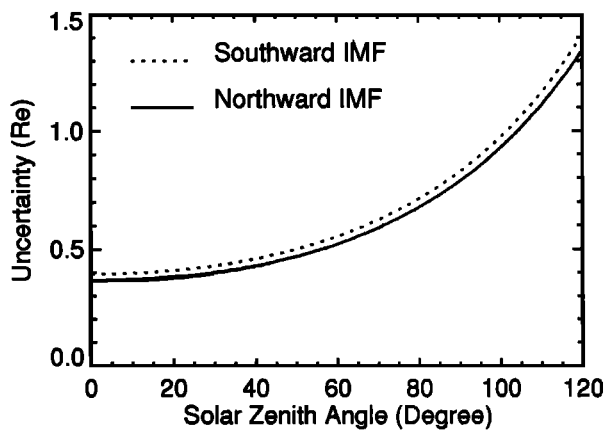

Figure 6. Uncertainty of the *Shue et al.* [1997] model versus solar zenith angle for southward and northward IMF.

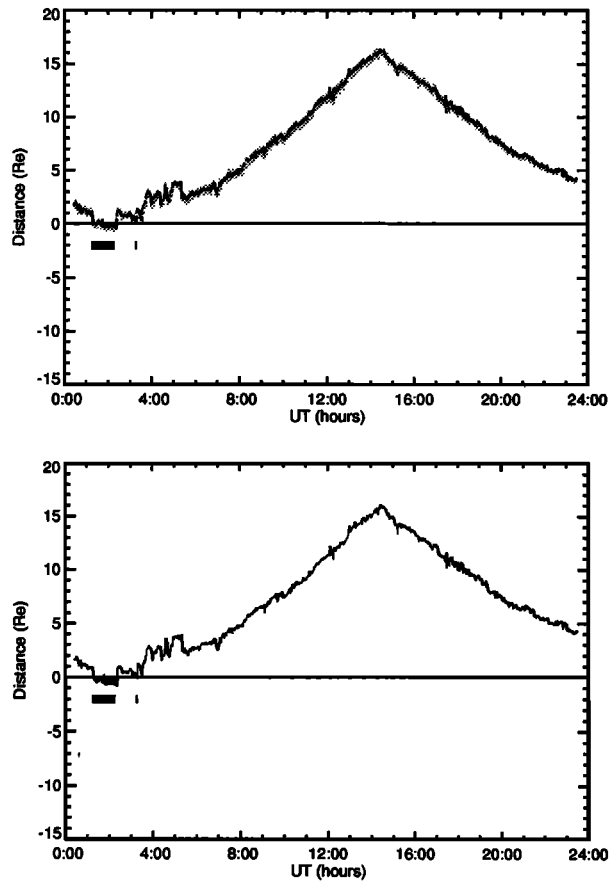

Figure 7. The distance from GMS 4 to the predicted magnetopause in the same format as Figure 5. (top) *Shue et al.* [1997]. (bottom) *Petrinec and Russell* [1996].

ing 1-4 min) into the magnetosphere at 0003, 0005, 0020, 0029, 0031, 0038, 0207, 0211, 0220, 0323, 0333, 0346, and 0428 UT, and finally entered the magnetosphere around 0547 UT. Although Geotail was mainly located in the magnetosheath during the interval 0355 through 0547 UT, it was closer to the magnetopause than it had been before 0355 UT because Geotail observed very short intervals (lasting less than ~1 min) of magnetospheric ions (above ~1 keV). Thick horizontal bars in Figure 8 show the magnetosheath intervals. In Figure 8, the *Shue et al.* [1997] prediction indicates that the distance changes sign from negative (solid region) to positive (white region) around 0543 UT. This change is consistent with the Geotail observations. *Petrinec and Russell* [1996] predict Geotail crossed the magnetopause at 0345 UT and moved back and forth between the magnetosphere and magnetosheath until 0541 UT. Their prediction is partially consistent with the Geotail observations.

Figure 9 is a similar plot for Interball 1. *Petrinec and Russell* [1996] predict the magnetopause location reasonably well. The magnetopause was within the error bar of the *Shue et al.* [1997] prediction; however, significant differences of the magnetopause crossing times indicate that *Shue et al.* [1997] needs improvement.

4. Improved Shue et al. Model

As shown in section 3, although the *Shue et al.* [1997] model does an excellent job in predicting Geotail crossings, it has significant room for improvement in order to predict Interball 1 crossings accurately. Here we recall that the model was derived bivariantly based on observations under average solar wind conditions. The complicated dependence on the two variants may lead to some peculiar behavior when we extrapolate it to extreme conditions. Figure 10 (top) shows the cross section of the magnetopause for $B_z = 17$ nT and various values of dynamic pressure for the *Shue et al.* [1997] model. The magnetopause flares rapidly when D_p is very high, which is peculiar as one would expect that the family curves evolve smoothly. We investigate the reason why this happens by replotting the observations (diamonds) and the linear fit of *Shue et al.* [1997] (dotted curves) in Figure 11. We find that the linear relationship extended to an extreme condition may exaggerate the relationship. For example, the subsolar standoff distance may approach zero when the IMF is extremely strong and southward, as shown by the dotted curve in the top plot of Figure 11.

To improve our model, we fit r_0 to a hyperbolic tangent function for B_z and fit α to a natural logarithmic

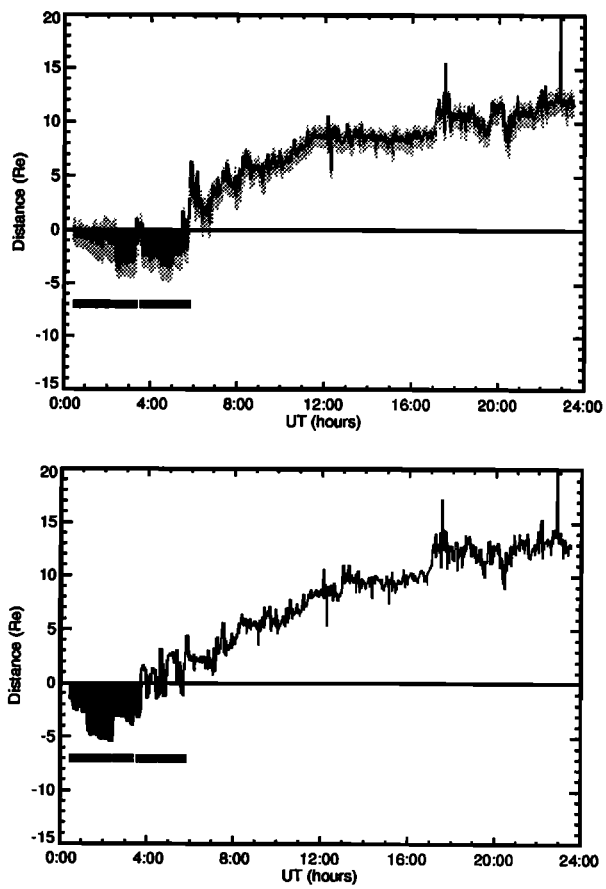

Figure 8. The distance from Geotail to the predicted magnetopause in the same format as Figure 5. (top) *Shue et al.* [1997]. (bottom) *Petrinec and Russell* [1996].

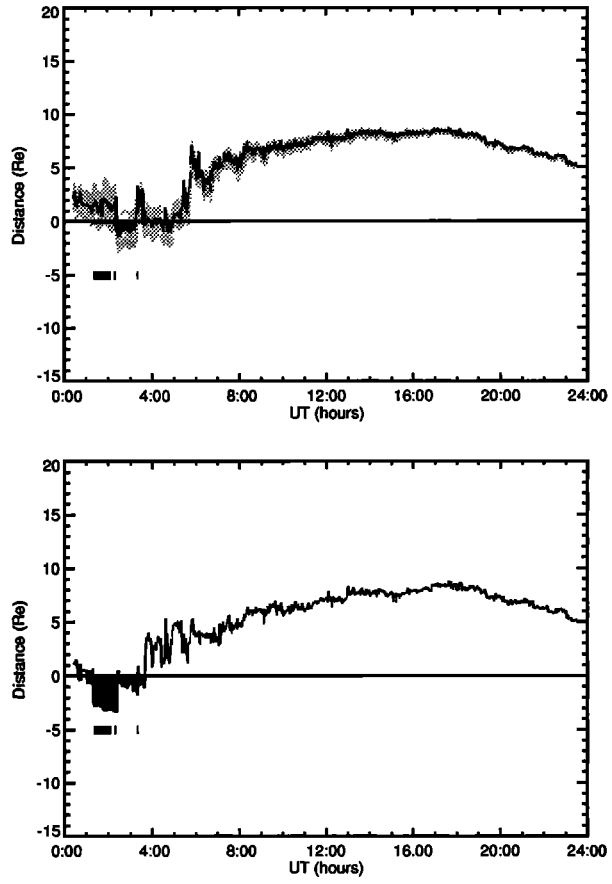

Figure 9. The distance from Interball to the predicted magnetopause in the same format as Figure 5. (top) *Shue et al.* [1997]. (bottom) *Petrinec and Russell* [1996].

function for D_p, which prevents r_0 and α from reaching unphysical values for extreme cases, as shown by the solid curves in Figure 11. Note that *Shue et al.* [1997] expressed the relationship for northward and southward IMF with two separate functions. The improved model only uses a single function to represent the r_0 dependence on B_z. The natural logarithmic function for α comes from substituting a power law of r_0 versus D_p into (1) and taking a natural logarithm of both sides of the equation to obtain $\alpha = A + B\ln(D_p)$, where A and B are the factors to be determined. Using the new nonlinear relationship, the best fit result gives

$$r_0 = 9.15 + 1.13\tanh[0.176(B_z + 7.31)], \quad (6)$$

$$\alpha = 0.59 + 0.022\ln(D_p). \quad (7)$$

Combining (6) and (7) with the (5) and (7) of [*Shue et al.*, 1997], we obtain

$$r_0 = \{a_1 + a_2\tanh[a_3(B_z + a_4)]\}(D_p)^{-\frac{1}{a_5}}, \quad (8)$$

$$\alpha = (a_6 + a_7 B_z)[1 + a_8\ln(D_p)], \quad (9)$$

where parameters a_1 through a_8 can be optimized using the gradient search technique [*Bevington*, 1969]. The initial seed values of these parameters are shown in the first column of Table 1. The final optimized values and uncertainties are shown in the second column of Table 1. The uncertainties are derived using the same Monte Carlo method used by *Shue et al.* [1997]. We have run multiple-parameter fittings 200 times using all dataset values which are sampled randomly each time, and points are allowed to be sampled repeatedly. We obtain 200 sets of coefficients and take their standard deviations as their uncertainties. The standard deviation between the analytic and the observed values for the improved model is 1.23 R_E. The final expressions for our improved model are

$$r_0 = \{10.22 + 1.29\tanh[0.184(B_z + 8.14)]\}(D_p)^{-\frac{1}{6.6}}, \quad (10)$$

$$\alpha = (0.58 - 0.007B_z)[1 + 0.024\ln(D_p)]. \quad (11)$$

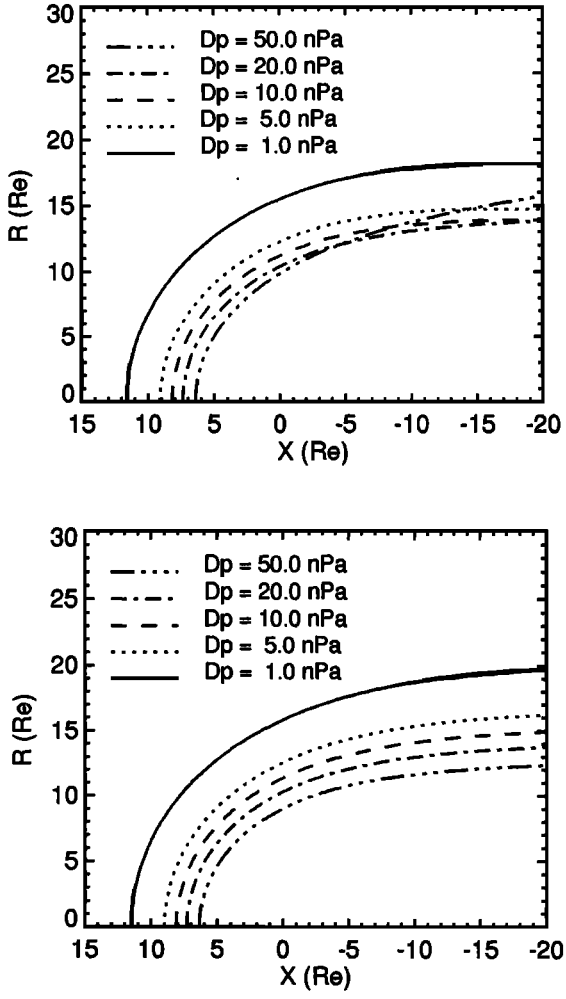

Figure 10. A demonstration of magnetopause locations as functions of D_p with a fixed B_z of 17 nT. (top) *Shue et al.* [1997]. (bottom) The improved Shue et al. model.

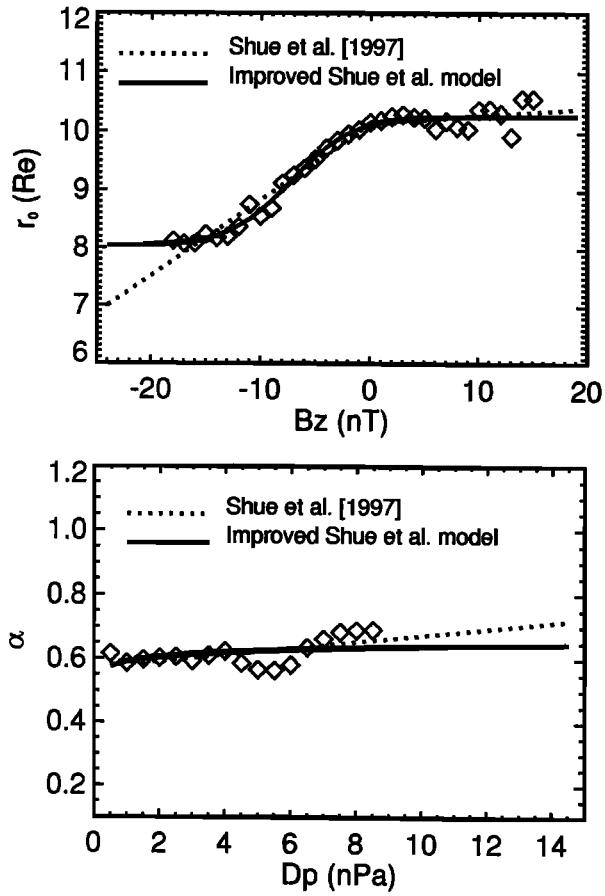

Figure 11. (top) Value r_0 as a function of B_z. (bottom) Value α as a function of D_p. The diamonds denote bin averages of r_0 and α derived from *Shue et al.* [1997] using magnetopause crossings. Dotted and solid curves represent the fitting results from *Shue et al.* [1997] and the improved Shue et al. model, respectively.

The improved Shue et al. model results are demonstrated in Figure 10 (bottom). The evolution of the magnetopause with D_p becomes smooth. Using this improved formula, we recalculate the distance from the predicted magnetopause to each satellite, as shown in Figure 12. The result leads to a significantly improved agreement with the observations, especially with the Interball 1 observations. Finally, we recalculate r_0 versus B_z and D_p in Figure 13. Comparing with the top plot of Figure 2, there is a significant change in the region for extremely southward IMF and the contours become smoother. Furthermore, the value of D_p needs to be at least 7 nPa in order for a geosynchronous satellite to have a magnetopause crossing, even when the IMF is extremely southward. This may be due to the limited

Table 1. Coefficients of Equations (8) and (9) Before and After the Multiple-Parameter Fit

	Before Fit (Seed Value)	After Fit
a_1	9.15	10.22 ± 0.10
a_2	1.13	1.29 ± 0.06
a_3	0.176	0.184 ± 0.007
a_4	7.31	8.14 ± 0.39
a_5	6.6	6.6 ± 0.5
a_6	0.59	0.58 ± 0.01
a_7	-0.010	-0.007 ± 0.0005
a_8	0.022	0.024 ± 0.0004

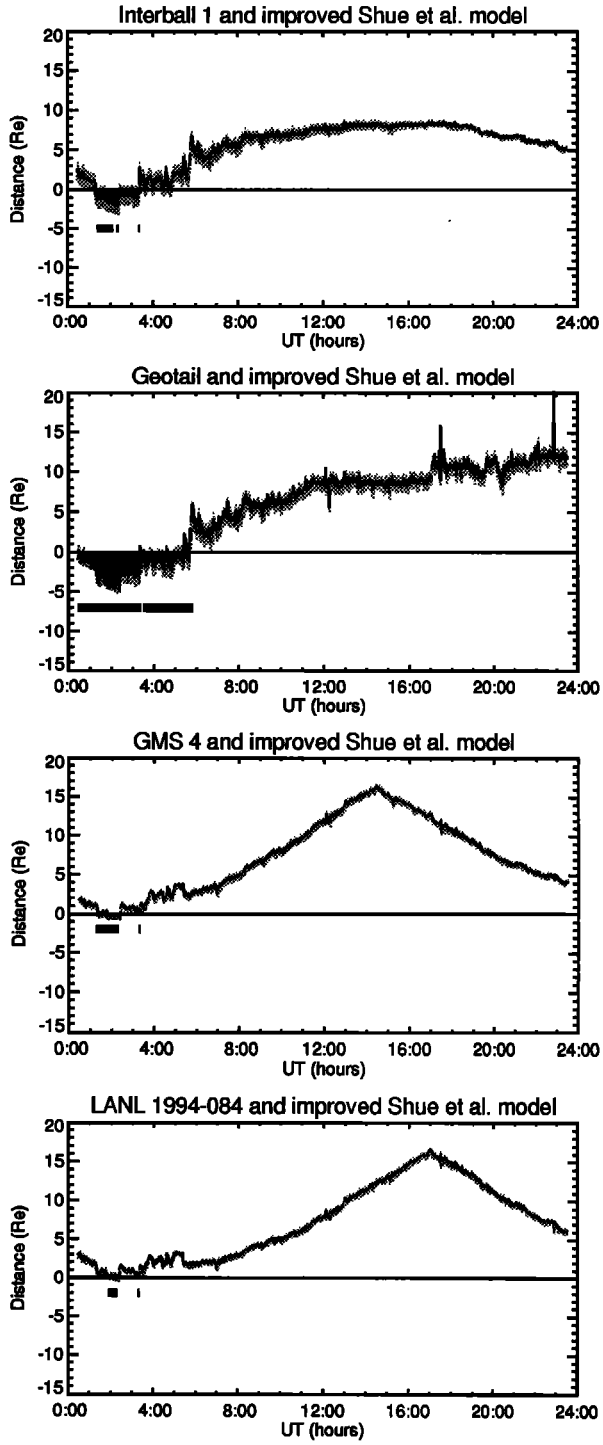

Figure 12. Distances between the prediction by the improved Shue et al. model to the Interball 1, Geotail, GMS 4, and LANL 1994-084 satellites in the same format as Figure 5.

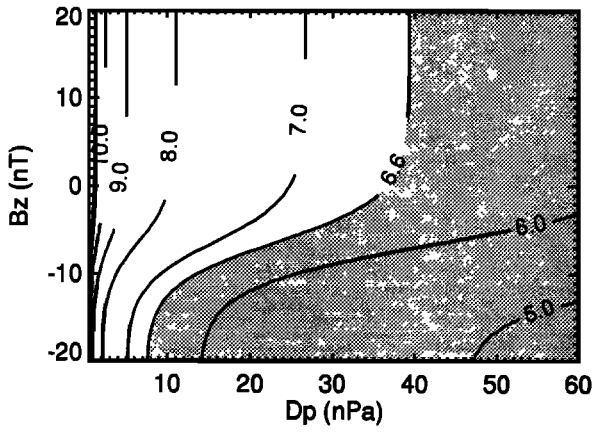

Figure 13. Standoff distance as functions of IMF B_z and solar wind dynamic pressure D_p derived from the improved Shue et al. model in the same format as Figure 3.

capability for reconnection to erode the magnetopause. *Kuznetsov and Suvorova* [1997] reported some magnetopause crossings at synchronous orbit. Their results are qualitatively consistent with our results, that is, a smaller D_p is needed to have a geosynchronous crossing when the IMF is southward than when the IMF is northward. However, quantitatively, the two results are different. We note that they used hourly averages of the solar wind measurements which tend to underestimate the peak values of solar wind parameters.

5. Discussion and Conclusions

The differences between the two models are caused by the following factors. First, the databases used in the two models are not the same. Second, the basic functional forms of the magnetopause location are different. The most important issue is how to handle the nightside magnetopause. The function used by *Petrinec and Russell* [1996] gives an open magnetopause on the nightside. *Shue et al.*'s [1997] functional form is mathematically simple and can model both the open and closed magnetosphere. This functional form provides the opportunity to describe how the magnetopause evolves with different IMF orientations. Furthermore, the specific dependence of the magnetopause on the upstream solar wind is different.

We have compared observations from several satellites with model predictions by *Shue et al.* [1997] and *Petrinec and Russell* [1996] for the January 11, 1997, event. During the January event, these two models correctly predict the magnetopause crossings on the dayside. It is therefore likely that either of these two models is able to provide a reasonably accurate warning of dayside magnetopause crossings for geosynchronous satellites. However, there are some differences in the predictions along the flank. The *Shue et al.* [1997] model correctly predicts the Geotail magnetopause crossings and partially predicts the Interball 1 crossings. The *Petrinec and Russell* [1996] model correctly predicts the Interball 1 crossings and is partially consistent with the Geotail observations.

The two models have treated the magnetopause as a rigid surface which responds to the upstream changes instantaneously. However, the real magnetopause is not rigid and will respond to the upstream changes dynamically, especially under extreme conditions. The magnetopause will oscillate around its equilibrium state. Therefore it is not expected that these models will predict precisely every single magnetopause crossing under such conditions. However, for the purposes of space weather forecasting, it is most important to predict that magnetopause crossings will occur and not the precise number of the crossings. As shown earlier, the level of the oscillations is similar to the error bar in the model. Therefore, for the space weather forecast, the magnetopause oscillation can be treated as a part of the error bar.

We have improved the *Shue et al.* [1997] model by introducing new functional forms to better represent the solar wind pressure effect on the magnetopause flaring and the IMF B_z effect on the subsolar standoff distance. The new functions provide a better implicit description of the underlying physical conservation laws and lead to a better agreement with the Interball 1 observations for this event.

Acknowledgments. This research was supported by Center of the Excellence (COE) program of Ministry of Education, Science, Culture, and Sports of Japan. The work at the University of Michigan was supported by NASA research grant NAGW-3948 and NSF grant ATM-9713492. The work at UCLA was supported by NASA under grant NAGW-3948 and by NSF under grant ATM 94-13081. The work at National Central University was supported by the National Science Council grant NSC 87-2111-M-008-008-AP8. G. Zastenker was partly supported by Russian Foundation for Basic Research by grant 95-02-03998. O. L. Vaisberg was supported in part under grant INTAS-93-2031. We would like to thank B. J. Thompson, M. Peredo, N. Fox, and other persons at NASA/GSFC who coordinated this event and collected related data for the ISTP homepage. We are grateful to R. P. Lepping for magnetic field measurements from WIND. Work at MIT was supported under NASA grant NAG5-2839. The authors would like to thank S. M. Petrinec for providing the program of his model. We want to thank E. C. Roelof and D. G. Sibeck for their comments. We also want to thank T. Mukai and Y. Saito of ISAS for using the LEP data from Geotail. We are indebted to K. K. Khurana for the program of multiple-parameter fit. We thank T. Obara of CRL for providing a list of crossings from GMS 4.

The Editor thanks T. Araki and another referee for their assistance in evaluating this paper.

References

Bevington, P. R., *Data Reduction and Error Analysis for the Physical Sciences*, McGraw-Hill, New York, 1969.

Chapman, S., and V. C. A. Ferraro, A new theory of magnetic storm, I, The initial phase, *J. Geophys. Res.*, *36*, 77, 1931.

Elsen, R. K., and R. M. Winglee, The average shape of the magnetopause: A comparison of three-dimensional global

MHD and empirical models, *J. Geophys. Res., 102*, 4799, 1997.

Fairfield, D. H., Average and unusual locations of the Earth's magnetopause and bow shock, *J. Geophys. Res., 76*, 6700, 1971.

Fairfield, D. H., Observations of the shape and location of the magnetopause: A review, in *Physics of the Magnetopause, Geophys. Monogr. Ser.*, vol. 90, edited by P. Song, B. U. Ö. Sonnerup, and M. F. Thomsen, p. 53, AGU, Washington D. C., 1995.

Ferraro, V. C. A., On the theory of the first phase of a geomagnetic storm: A new illustrative calculation based on idealized (plane not cylindrical) model field distribution, *J. Geophys. Res., 57*, 15, 1952.

Formisano, V., V. Domingo, and K.-P. Wenzel, The three-dimensional shape of the magnetopause, *Planet. Space Sci., 27*, 1137, 1979.

Gosling, J. T., M. F. Thomsen, S. J. Bame, R. C. Elphic, and C. T. Russell, Observations of reconnection of interplanetary and lobe magnetic field lines at the high-latitude magnetopause, *J. Geophys. Res., 96*, 14,097, 1991.

Howe, H. C., and J. H. Binsack, Explorer 33 and 35 plasma observations of magnetosheath flow, *J. Geophys. Res., 77*, 3334, 1972.

Kartalev, M. D., V. I. Nikolova, V. F. Kamenetsky, and I. P. Mastikov, On the self-consistent determination of dayside magnetopause shape and position, *Planet. Space Sci., 44*, 1195, 1996.

Kuznetsov, S. N., and A. V. Suvorova, Magnetopause shape near geostationary orbit (in Russian), *Geomagn. Aerono., 37*(3), 1, 1997.

Petrinec, S. M., and C. T. Russell, An empirical model of the size and shape of the near-Earth magnetotail, *Geophys. Res. Lett., 20*, 2695, 1993.

Petrinec, S. M., and C. T. Russell, Near-Earth magnetotail shape and size as determined from the magnetopause flaring angle, *J. Geophys. Res., 101*, 137, 1996.

Petrinec, S. M., P. Song, and C. T. Russell, Solar cycle variations in the size and shape of the magnetopause, *J. Geophys. Res., 96*, 7893, 1991.

Roelof, E. C., and D. G. Sibeck, Magnetopause shape as a bivariate function of interplanetary magnetic field B_z and solar wind dynamic pressure, *J. Geophys. Res., 98*, 21,421, 1993.

Shue, J.-H, J. K. Chao, H. C. Fu, C. T. Russell, P. Song, K. K. Khurana, and H. J. Singer, A new functional form to study the solar wind control of the magnetopause size and shape, *J. Geophys. Res., 102*, 9497, 1997.

Sibeck, D. G., R. E. Lopez, and E. C. Roelof, Solar wind control of the magnetopause shape, location, and motion, *J. Geophys. Res., 96*, 5489, 1991.

Song, P., and C. T. Russell, Model of the formation of the low-latitude boundary layer for strongly northward interplanetary magnetic field, *J. Geophys. Res., 97*, 1411, 1992.

Song, P., R. C. Elphic, and C. T. Russell, ISEE 1 and 2 observations of the oscillating magnetopause, *Geophys. Res. Lett., 15*, 744, 1988.

Sotirelis, T., The shape and field of the magnetopause as determined from pressure balance, *J. Geophys. Res., 101*, 15,255, 1996.

Thomsen, M. F., J. E. Borovsky, D. J. McComas, R. C. Elphic, and S. Maurice, The magnetospheric response to the CME passage of Jan. 10-11, 1997, as seen at geosynchronous orbit, *Geophys. Res. Lett.*, in press, 1998.

J.K. Chao, Institute of Space Science, National Central University, Chungli 32054, Taiwan. (e-mail: T272362@twncu865.ncu.edu.tw)

T.R. Detman and H.J. Singer, Space Environment Center, NOAA R/E/SE, 325 Broadway, Boulder, CO 80303-3328. (e-mail: tdet@sec.noaa.gov; hsinger@sec.noaa.gov)

H. Kawano, Department of Earth and Planetary Sciences, Kyushu University 33, 6-10-1 Hakozaki, Higashiku, Fukuoka, Fukuoka 812-8581, Japan. (e-mail: hkawano@geo.kyushu-u.ac.jp)

S. Kokubun and J.-H. Shue, Solar-Terrestrial Environment Laboratory, Nagoya University, Toyokawa, Aichi 442-8507, Japan. (e-mail: kokubun@stelab.nagoya-u.ac.jp; jhshue@stelab.nagoya-u.ac.jp)

C.T. Russell, Institute of Geophysics and Planetary Physics, University of California, Los Angeles, 6877 Slichter Hall, Los Angeles, CA 90095-1567. (e-mail: ctrussel@igpp.ucla.edu)

P. Song, Space Physics Research Laboratory, University of Michigan, 2455 Hayward Street, Ann Arbor, MI 48109-2143. (e-mail: psong@engin.umich.edu)

J.T. Steinberg, Center for Space Research, Massachusetts Institute of Technology, Cambridge, MA 02139. (e-mail: jts@space.mit.edu)

O.L. Vaisberg and G. Zastenker, Space Research Institute, Russian Academy of Sciences, 84/32 Profsoyuznaya, 117810 Moscow, Russia (e-mail: olegv@iki.rssi.ru; gzastenk@arc.iki.rssi.ru)

(Received December 15, 1997; revised March 5, 1998; accepted March 25, 1998.)